Reflight of the Stratospheric Terahertz Observatory: (STO-2)

An LDB Experiment to Investigate the Life Cycle of the Interstellar Medium

1 Executive Summary

The structure of the interstellar medium, the life cycle of interstellar clouds, and their relationship with star formation are processes crucial to deciphering the internal evolution of galaxies. High resolution spectral line imaging of key gas tracers not accessible from the ground is needed to fill in major missing pieces of Galactic structure and witness the formation and dissipation of interstellar clouds. The reflight of the Stratospheric Terahertz Observatory (STO-2), a balloon-borne 0.8-meter telescope with an 8-beam far-infrared heterodyne spectrometer, will address these issues and significantly advance NASA's Strategic Goal of "discovering how the universe works" by exploring how structures in galaxies evolve and how global star formation proceeds.

In its long duration flight, STO-2 will survey part of the Galactic plane in [C II] line emission at 158 μm, the brightest spectral line in the Galaxy; and [N II] line emission at 205 μm, a tracer of the star formation rate. At ~1' angular resolution and <1 km/s velocity resolution, STO-2 will detect every interstellar cloud with $A_V \geq 0.4$ in the surveyed region (Figure 1), and, through excitation and kinematic diagnostics provided by [C II] and [N II] line emission, will study how atomic and molecular clouds are formed and dispersed in the Galaxy. STO-2 will make 3-dimensional maps of the structure, dynamics, turbulence, energy balance, and pressure of the Milky Way's Interstellar Medium (ISM), as well as the star formation rate.

The first flight of STO in January 2012 provided an initial look at [CII] emission from selected regions, several [CI] maps, and a modest number of CO J=12-11 detections. STO-2 will greatly profit from the technical lessons learned from STO-1, and will build on the scientific returns of STO-1. This summary section briefly describes science goals, mission approach, and complementarity with other missions; subsequent sections 2-4 go into more detail on each topic.

1.1 Summary: Science Goals and Objectives

STO-2 will provide a comprehensive understanding of the inner workings of our Galaxy by exploring the connection between star formation and the life cycle of interstellar clouds. We will study the formation of molecular clouds, the feedback of high mass star formation heating and disrupting clouds, and the effect of these processes upon the global structure and evolution of the Galaxy. The detailed understanding of star formation and evolution of stars and gas in the Galaxy is directly relevant to star formation in other galaxies. The nature of the feedback mechanism of massive star formation is pivotal to the evolution of galaxies. STO-2 thus addresses NASA's goals and research objectives on galaxy evolution and star formation. STO-2 addresses the high priority goals:

1. Determine the life cycle of Galactic interstellar gas.
2. Study the creation and disruption of star-forming

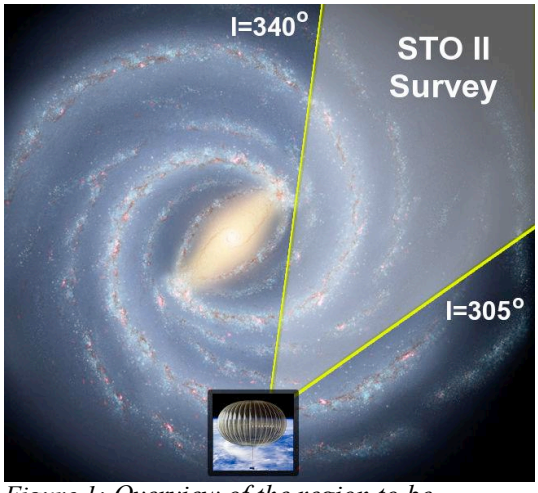

Figure 1: Overview of the region to be surveyed by STO-2. This 35° longitudinal swath of the Galactic Plane reveals major components of the Milky Way ISM, such as the molecular ring, the Scutum-Crux spiral arm, and the interarm region.

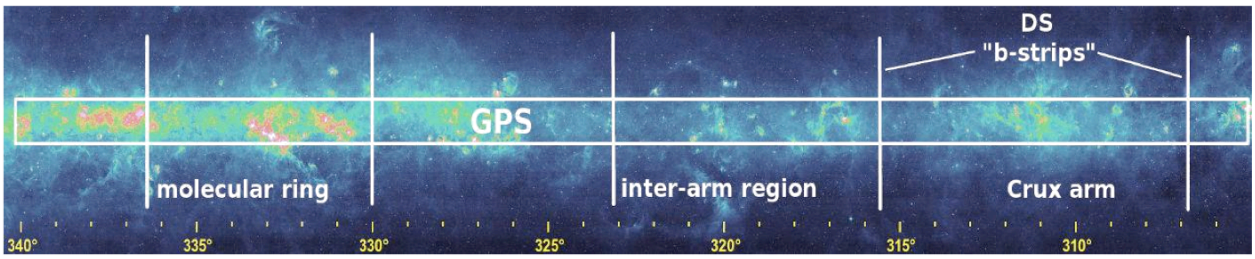

Figure 2: *Midcourse Space Experiment (MSX) 8.3 μm map of the Galactic Plane from the Molecular Ring through the Scutum-Crux spiral arm. Annotations highlight regions to be explored by STO-2.*

clouds in the Galaxy.

3. Determine the parameters that affect the star formation rate in a galaxy.
4. Provide templates for star formation and stellar/interstellar feedback in other galaxies.

1.2 Summary: Mission Approach

To achieve these scientific goals, STO-2 will map the pivotal [C II] 158 μm and [N II] 205 μm lines. In particular, **[C II] is extraordinarily versatile**; it probes ionized gas (HII), atomic clouds (HI), and the photo-illuminated surfaces of molecular clouds. **[C II] provides a unique measure of the interstellar medium that is not possible with HI or CO line emission alone**: it directly distinguishes *atomic clouds* from diffuse HI gas, identifies "dark" molecular gas not associated with CO emission, and is integral to measuring the formation and destruction of clouds that is not disentangled from HI maps and not probed by CO. The [N II] line, in addition to providing an extinction-free probe of ionizing radiation and star formation rate in the Galaxy, can be used to isolate the fraction of [C II] line emission that comes from ionized gas, conclusively determining its origin and distribution.

To map the [C II] and [N II] lines over a large portion of the Galactic Plane, STO-2 will utilize two heterodyne receiver arrays to produce a total of eight beams in the focal plane, each with 1024 spectral channels. In the long duration (14-28 day) flight STO-2 will map a 35 square degree area including the Galactic molecular ring (Figures 1 & 2) as well as 5 deeper strips in Galactic latitude b=±2° in selected arm and interarm regions. STO-2 achieves 1 arcminute spatial resolution and 3σ intensity limits of 2.0×10^{-5} (t/1 sec)$^{-1/2}$ and 8.0×10^{-6} (t/1 sec)$^{-1/2}$ erg s^{-1} cm^{-2} sr^{-1} in the [C II] and [N II] lines – sufficient to detect and resolve both spectrally and spatially all Giant Molecular Clouds (GMCs), all significant H II regions, and all cold neutral medium (CNM) clouds with $A_V \geq 0.4$ mag (potential building blocks of GMCs) in the surveyed region. The STO-2 heterodyne receivers provide sub-km/s velocity discrimination and sufficient bandwidth to detect and resolve line emission from all Galactic clouds along the line of sight. The deliverable data products include:

1. A high fidelity database of spatially and velocity resolved far-infrared [C II] 158 μm and [N II] 205 μm fine-structure line emission in the Galaxy.
2. A combination of STO-2's data products with existing line and continuum surveys to characterize the structure and dynamics of interstellar clouds and their relation to star formation.

The data are produced in large scale (Galactic Plane Survey) and selective (Deep Survey) modes:

- **GPS: Galactic Plane Survey:** $305° < l < 340°$; $-0.5° < b < 0.5°$. The GPS contains more than 10^5 spatial pixels and has 10^4 times higher sensitivity than FIRAS/COBE when convolved to the same resolution. STO-2 will catalogue all neutral clouds with $A_V \geq 0.4$ mag. and all ionized clouds with emission measure > 50 cm^{-6} pc.
- **DS: Deep Survey** of arm and interarm regions defined by ancillary observations from AST/RO and

Mopra telescopes: $b = -2^\circ$ to $+2^\circ$ strips at $l = 315.97^\circ$, 323.13°, 330.00°, 336.42° and 342.54°, with $\Delta b = 0.05^\circ$. Sensitivity will be 3-4 times higher than the Galactic Plane Survey.

1.4 Summary: Complementarity with Other Missions and Existing Data

STO-2 is timely. STO-2 will provide the best corresponding interstellar cloud survey to the GLIMPSE and MIPSGAL Spitzer Legacy programs, the Herschel Infrared Galactic Plane Survey HIGAL, and H I and CO line surveys. STO-2 will enhance the interpretation of these data sets by completing the observational links required to trace the cloud life cycle. Using Galactic rotation to place the clouds along the line of sight, STO-2's high spectral resolution enables 3 dimensional maps of Galactic interstellar matter, from which many physical parameters in the Galaxy (e.g., pressure and star formation rate) can be extracted.

STO-2, being optimized for large-scale mapping of the weak extended emission of ISM clouds, complements the high angular resolution, but limited mapping capabilities of contemporary far-IR platforms with heterodyne receivers. The larger *Herschel Space Observatory* (HSO) and the *Stratospheric Observatory for Infrared Astronomy* (SOFIA) have beam sizes of 12 to 15″ at [CII], and mapping speeds that are 2-3 orders of magnitude slower than STO-2.

STO-2 builds on the technical lessons (see §6) and results (see §1.x) from the STO-1 flight. STO-1 obtained drift scans of [CII] and CO J=12-11 toward the bright star forming regions NGC 3576 and η Carina, as well as near the $l = 342.54^\circ$ b strip and the GMC G328.1 (see §2.2, 3 and 5.2). STO-1 also made 15′x15′ [CI] maps of NGC 3576, η Carina, and G328.1, as well as mapping the b strip from -1° to $+1^\circ$ at $l = 342.54^\circ$ in [CI]. These results serve as stepping stones to the much more extensive [C II] and [N II] surveys of STO-2.

2 Science Goals & Objectives

2.1 Background

Via spatially and spectroscopically resolved [C II] and [N II] line emission, STO-2 probes the formative and disruptive stages in the life cycles of interstellar clouds. It reveals new insight into the relationship between interstellar clouds and the stars that form from them, a central component of galactic evolution.

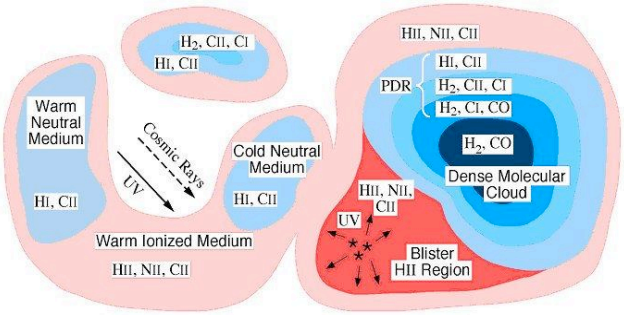

Figure 3: *Schematic representation of ISM components. STO-2 detects and maps in the Galaxy the higher column density CNM component, the H_2/C^+ "dark" component, the photodissociation region (PDR) surfaces of molecular clouds, the H II component, and (with H I) the WNM/CNM ratio.*

Neutral interstellar gas is the dominant mass component of the ISM, and tends to exist as two phases in rough thermal pressure equilibrium: a diffuse warm neutral medium (WNM) with hydrogen densities at the solar circle of $n \sim 0.3$ cm^{-3} and T~8000 K, and denser, colder "diffuse HI clouds" (CNM) with n ~40 cm^{-3} and T~70 K (Heiles & Troland, 2003; Wolfire et al., 2003). Turbulence provides a broader spectrum of conditions (Mac Low et al., 2005; Gazol et al., 2005; Jenkins & Tripp, 2011), but thermal balance drives neutral gas toward these phases. With sufficient shielding column, $N > 10^{20} - 10^{21}$ cm^{-2} of hydrogen nuclei, the CNM clouds begin to harbor molecular interiors. These H_2/C^+ clouds are sometimes called "dark clouds" because they cannot be detected in HI, H_2, or CO emission. This component has been indirectly inferred by γ ray (e.g., Grenier et al. 2005), submillimeter dust emission (Planck Collaboration et al. 2011), and IR dust extinction maps, but direct emission from its gas in [CII] and accurate measurement of its contribution to the ISM and to the formation of GMCs can be done only by STO-2. Above $N \sim 3 \times 10^{21}$ cm^{-2} the clouds become detectable in CO, and above $N \sim 10^{22}$ cm^{-2} they become gravitationally bound and stars may form

in their interiors (McKee, 1989). The largest condensations take the form of GMCs with masses $10^5 - 10^6$ $M_\odot$ and are responsible for most of the star formation in the Galaxy. These ISM components are shown schematically in Figure 3.

WNM is converted into CNM clouds via thermal instability either if the ultraviolet radiation field (heating) diminishes (Parravano et al., 2003) or if the pressure increases because of the passage of a (e.g., super-nova) shock wave (McKee & Ostriker, 1977). GMCs presumably form from a large assemblage of CNM clouds; the leading theoretical models invoke gravitational instabilities in huge regions 0.5-1 kpc in size along spiral arms (Ostriker & Kim, 2004). This assemblage process has never been directly observed and other mechanisms have been invoked such as the convergence of flows in a turbulent medium (Hennebelle & Perault, 2000; Heitsch et al., 2006).

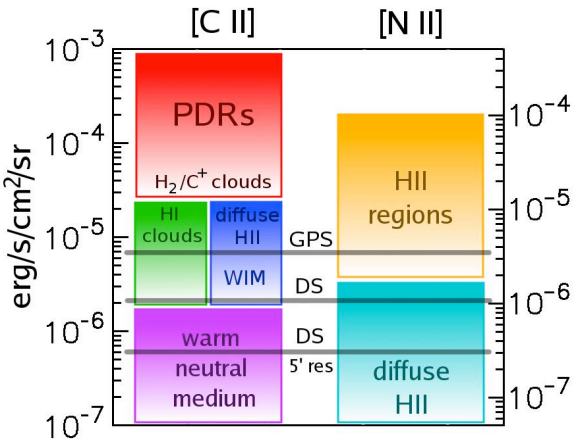

Figure 4: *Comparison of STO-2's sensitivity with [C II] and [N II] integrated intensity for various ISM components. HI and H_2/C^+ clouds (dark gas) constitute the building blocks for molecular clouds. HII regions and bright PDRs often constitute photoevaporating gas from molecular clouds, or cloud destruction. The corresponding sensitivities (3σ rms noise) of STO-2's two survey modes (see §1.2 for definitions) are indicated by horizontal lines.*

The ultraviolet radiation from massive stars not only heats the CNM and WNM and determines the rela-tive portions of these phases, but it also ionizes gas and heats it to 10^4 K, producing H II (low density=WIM) regions. [N II] line emission provides an extinction-free measure of ionizing radiation from young, massive stars (a direct measure of star formation rates), and [C II] and [N II] together measure the disruptive impact of UV radiation on the surfaces of neighboring clouds; a key part of the stellar/interstellar feedback that governs galactic evolution. GMCs are primarily destroyed by the ultraviolet radiation from OB stars which form inside and lie relatively close to their natal GMCs (Williams & McKee, 1997). CNM clouds are destroyed by the interstellar UV field produced by the global (many hundreds of pc) OB stellar population. A high global star formation rate produces a more intense interstellar radiation field, thereby lowering the CNM population and converting these regions to ionized or WNM gas. This conversion then lowers the rate of GMC formation, and thus the global star formation rate. These stellar feedback effects could regulate star formation rates in galaxies.

Figure 4 shows the [C II] and [N II] intensities of these cloud components with the nominal STO-2 survey mode sensitivities, while Figure 5 shows a Herschel/GOTC+ [C II] observation (see also §4.2) with complementary CO and H I spectra along a line of sight through the Galaxy. This pointed observation shows that many kinds of clouds are detectable with modern heterodyne receivers at THz frequencies. Diffuse clouds appear with [C II] and HI emission, whereas illuminated surfaces of molecular clouds are visible in [C II] and CO. A significant WNM component is observed in the HI (only). This single-pointing with Herschel foreshadows the large-scale mapping of these lines that will be possible with STO-2.

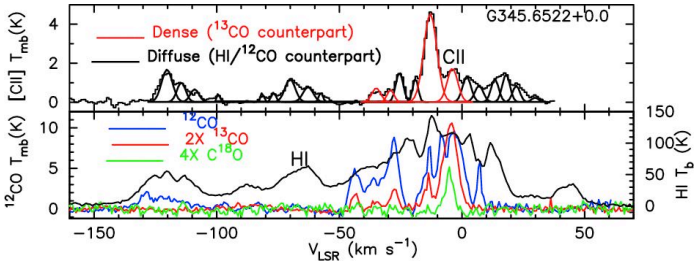

Figure 5: *[C II] spectra obtained with Her-schel/HIFI for the GOTC+ program (Langer et al. 2010), along with CO and HI data, show that many different types of interstellar clouds can be observed along a single line of sight in the Galaxy.*

2.2 Goal 1: Map the Entire Life Cycle of Interstellar Gas

STO-2 will (1) map and catalog as a function of Galactic position the size, mass distribution and internal velocity dispersion of atomic, molecular and ionized clouds in the Galaxy. It will (2) identify the physical origin of [C II] emission, (3) allow construction of the first large-scale thermal pressure map of the ISM, (4) the first map of the gas heating rate, and (5) a more sensitive, detailed map (using [N II]) of the star formation rate.

(1) Interstellar gas cycles from molecular gas, to atomic and ionized gas, and back to molecular gas. STO-2's unique blend of sensitivity, angular resolution and spectral resolving power allows it to map and diagnose *all components of the warm and cold interstellar medium*. STO-2 will survey spiral arm, interarm regions and a large portion of the molecular ring, where much of the star formation occurs in the Galaxy. Galactic rotation causes a distance-dependent velocity separation of the clouds along the line of sight, and STO-2's high spectral resolution allows us to then determine the distance to the clouds (there is a "near" and "far" solution, but this distance ambiguity can be solved by standard methods). Therefore, *STO-2 will provide an unprecedented 3D global map of the distribution of clouds of ionized gas, atomic gas, and molecular clouds (via their dense atomic surfaces) as a function of Galactocentric radius (R) and height (z) in the Galaxy*. We can compute the density of clouds (i.e., the number of clouds per kpc^3) and their size distribution as functions of R and z, and see how clouds are clumped together in spiral arms or supershells. In regions of cloud clustering, the superb velocity resolution of STO-2 will measure the random motions of clouds, and diagnose *large scale turbulence*.

Where extended emission is seen in H I with no [C II] counterpart in the GPS, we can attribute the H I emission to extended low density gas – either WNM or thermally unstable gas with densities below that of CNM (Figure 4). To achieve the required sensitivity to detect highly extended diffuse gas in the DS, we will smooth the data to corresponding larger spatial and spectral bins. In this way, STO-2 can map the CNM/WNM mass fraction in the Galaxy, and determine how much of the neutral gas is in clouds rather than in warm or unstable components. This ratio can be correlated to the thermal pressure, to the ultraviolet radiation field, and to the star formation rate to probe the stellar feedback processes that regulate star formation.

(2) Because [C II] line emission can come from ionized, atomic, and molecular gas, its origin can be difficult to disentangle toward complicated lines of sight, particularly in the Inner Galaxy. For example, COBE FIRAS observations show that the ionized component of the ISM radiates strongly in both [C II] 158 μm and [N II] 205 μm (Wright et al., 1991). To distinguish the origin(s) of [C II] emission, velocity-resolved measurements of the distribution of the ionized gas must be made in [N II] and compared to the [C II] distribution. *STO-2 will conclusively determine the origin of the [C II] emission*, and will enable the portion of the [C II] emission coming from the CNM neutral gas to be unambiguously determined.

(3) If the CNM clouds are seen in H I, which determines their column and mass, the ratio of CNM [C II] to H I intensity provides a measure of the [C II] emissivity per H atom which rises monotonically with gas density and thermal gas pressure. *The STO-2 survey over a large portion of the Galactic Plane thereby enables the construction of the first barometric maps of the Galactic disk*, determining the ambient thermal pressure in different environments (e.g., the spiral arms versus interarm regions, turbulent versus quiescent regions). The STO-2 team's theoretical models are vital to determining the density, temperatures, and thermal pressures in the clouds. These can then be correlated with star formation rates to understand stellar/interstellar feedback mechanisms.

(4) The [C II] line dominates the cooling of CNM clouds. From its intensity we directly obtain the gas heating rate of clouds as a function of radius throughout the Galaxy. Besides the fundamental interest in tracing the energy flow in the Galaxy, the observations also can test our theoretical hypothesis that the heating is provided by the grain photoelectric heating mechanism in diffuse clouds. This hypothesis has

been tested (positively) in denser clouds illuminated by stronger fields, but in weak UV fields other mechanisms may be important.

2.3 Goal 2: Reveal the Formation & Destruction of Clouds

By observing the [C II] line, STO-2 will reveal clouds clustering and forming in spiral arms, super-shells, and filaments, and follow the growth of clouds to shield molecules and eventually to become gravitationally-bound giant molecular clouds (GMCs). STO-2 will observe "dark" gas that has no counter-part in HI or CO emission, measure its contribution to GMC formation. STO-2 will also directly measure the subsequent dissolution of molecular clouds into diffuse gas via stellar feedback.

Formation of diffuse HI clouds (CNM). Turbulence may play an important role in the formation and evolution of interstellar clouds. In a standard scenario where CNM clouds are formed from WNM gas by thermal instability, we can picture the role of turbulence in two ways: large scale instabilities, density waves and supernovae drive compressional motions that increase the thermal pressure and trigger the thermal instability (de Avillez & Breitschwerdt, 2005). Alternatively, regions undergoing thermal instability may generate turbulence, and convert the CNM into a complex network of pancakes and filaments (Kritsuk & Norman, 2002). Because of this dynamic nature of both the triggering and evolution of the thermal instability, departures from thermal pressure equilibrium may be widespread in the ISM (Heiles & Troland, 2003), and the notion of a dynamic multiphase ISM has been proposed. Only a careful study of both the spatial structure and kinematics of diffuse gas in transition between phases can tell us the role of turbulence and dynamic pressure in the life-cycle of the ISM.

Formation of GMCs. The formation of GMCs is a prerequisite for star formation, yet the process has not yet been directly observed! STO-2 is designed with the unique combination of sensitivity and resolution needed to observe cold atomic and dark clouds assembling GMCs (Figure 6).

Four mechanisms have been proposed to consolidate gas into GMC complexes (Elmegreen 1996): (1) self-gravitating instabilities within the diffuse gas component (often in a spiral arm where density is highest and the Jeans time is shortest), (2) random collisional agglomeration of clouds, (3) accumulation of material within high pressure environments such as shells and rings generated by OB associations, and (4) compression in the randomly converging parts of a turbulent medium. STO-2 can distinguish these processes from each other and consider new cloud formation schemes by:

- Accounting for all the molecular hydrogen mass (the H_2/C^+ dark clouds as well as the H_2/CO clouds) when computing global measures of the interstellar medium.
- Clearly identifying CNM clouds via the density sensitivity of [CII] compared to H I 21 cm.
- Constructing spatial and *kinematic* comparisons with sufficient resolution, spatial coverage and dynamic range to discriminate the above 4 scenarios.

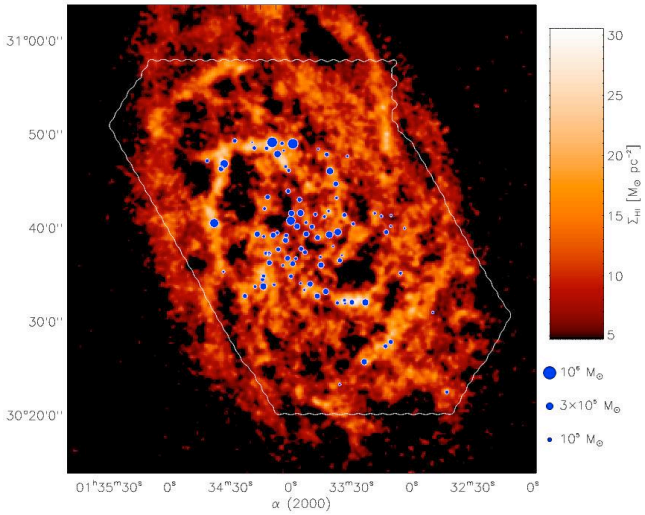

Figure 6: *The location of GMCs (blue dots) in the nearby spiral galaxy M33 are overlaid upon an integrated intensity map of the HI 21 cm line (Engargiola et al., 2003). These observations show that GMCs in M33 are formed from large structures of atomic gas, and foreshadow the detailed study of GMC formation that STO-2 provides in the Milky Way.*

Currently, associating diffuse gas (H I) with molecular gas (CO) is difficult owing to the density-insensitivity of the HI 21cm line. Unlike [C II], a significant fraction of the H I emission can come from low density WNM gas. Because the [C II] emissivity is 10 times higher for HI clouds than WNM gas, it barometrically picks out clouds of atomic CNM gas. It directly detects and weighs the dark gas, and reveals its motion. Regions of GMC formation may therefore be tracked by higher than average HI and H_2/C^+ cloud densities (number of clouds per kpc^3), or regions with individual clouds with higher than average columns or pressures. With STO-2's velocity resolution, these regions can be identified with superrings or spiral arms or convergent parts of a turbulent medium. STO-2 will identify the sequence of phase transitions as the gas transits through the spiral potential, and *will witness the process of cloud formation* directly from HI or dark gas clouds. For example, dust lanes along the inner edges of spiral arms often show neither H I nor CO emission (Wiklind et al., 1990; Tilanus & Allen, 1991), and are therefore likely to be dark gas (Grenier et al. 2005, also Figure 3) that will be seen in [C II] by STO-2.

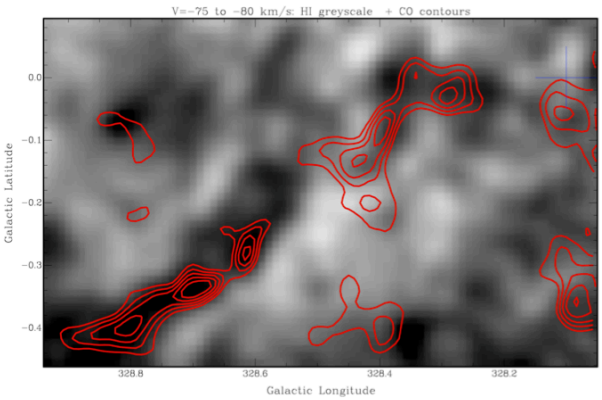

Figure 7: *An example of a young GMC filament (50 pc long at a distance of* ~4.5 *kpc with mass* ~5×10^5 $M_\odot$*). Mopra CO J=1-0 contours (red) are overlaid on an HI 21 cm image. A blue cross marks the line of sight of a single Herschel GOT* C^+ *(see §4.2) observation, which uncovered bright [CII]. An STO-2 [CII] map of this region will much more clearly show the kinematics and the location of the atomic and "dark" clouds that may be coalescing to form this GMC.*

One example of such a candidate cloud-forming region is shown in Figure 7, where high-resolution CO J=1-0 observations from Mopra (§5.1) are overlaid upon a HI map from SGPS (McClure-Griffiths et al., 2005). A 50 pc GMC filament of CO emission is shown over a narrow (5 km/s) velocity interval along with the same velocity HI; the region also shows an absence of bright infrared continuum features. While these observations are generally consistent with a natal GMC that has not yet evolved to form dense cores or young stars, imaging spectroscopy of [CII] from STO-2 would *provide conclusive evidence for GMC formation*. Unlike HI observations alone, [CII] emission can easily distinguish dense clouds of HI from diffuse gas, and can reveal dark clouds. Furthermore, with high spectral resolution, the atomic and molecular kinematics of GMC assembly can be directly measured with high fidelity from the [CII], HI, and CO line profiles.

The high spectral resolution of STO-2 enables crucial kinematic studies of the Galaxy to be made. The expansion of stellar outflows and supernova remnants create supershells that sweep up surrounding ISM and overrun surviving molecular clouds and cloud fragments. STO-2 will determine the kinematics and thermal pressures of most supershells, fossil superrings, and molecular clouds just condensing via gravitational instability of old superrings. STO-2 will detect many of the CNM clouds formed out of WNM in the shells, and the larger column density clouds, which may harbor H_2. With these detections STO-2 will determine the role of OB association-driven supershells and superrings in the production of molecular clouds and the cycling of gas between the various phases of the ISM.

STO-2 witnesses the disruption of clouds. [C II] and [N II] measure the photoevaporating atomic or ionized gas driven from clouds with UV-illuminated surfaces, thereby converting the clouds to WNM or to diffuse H II regions. Thus, STO-2 can directly determine the rate of mass loss from catalogued clouds, and their destruction timescales.

2.4 Goal 3: Map the Star Formation Rate in the Galaxy

STO-2 will probe the relation between the gas surface density on kpc scales and the [N II]-derived star formation rate, so that we might be able to better understand the empirical Schmidt Law used to estimate the star forming properties of external galaxies.

Star formation within galaxies is commonly described by two empirical relationships: the variation of the star formation rate per unit area with the gas surface density (atomic + molecular), Σ_{SFR} (Schmidt, 1959) and a surface density threshold below which star formation is suppressed (Kennicutt, 1989; Martin & Kennicutt, 2001). The Schmidt Law has been evaluated from the radial profiles of Hα, H I, and CO emissions for tens of galaxies. The mean value of the Schmidt index, n, is 1.3 ± 0.3 (Kennicutt, 1989), valid for kpc scales. This empirical relationship is used in most models of galaxy evolution with surprising success given its simplicity. Oddly, there has been little effort to evaluate the Schmidt Law in the Milky Way owing to the difficulty in deriving the star formation rate, and a complete census of gas surface density, as a function of radius within the plane.

The STO-2 survey of [C II] and [N II] emission provides the optimum data with which to calculate the Schmidt Law in the Milky Way. The [N II] line is a potentially excellent tracer of the star formation rate, measuring ionizing luminosity with high sensitivity, angular and spectral resolution, and being unaffected by extinction. The [C II] line, in conjunction with H I 21-cm and CO line emissions, provide the first coherent map of the neutral interstellar gas surface density and its variation with radius.

STO-2 may help us understand the origin of the Schmidt Law. For example, it will correlate the thermal pressures on the surfaces of GMCs (which may relate to the star formation rate inside) with surface densities of H I and CO. It may uncover regions around OB associations devoid of GMC-forming CNM clouds. The current high rate of star formation in associations may impoverish large regions of the clouds needed to start the star formation cycle in the future. Such measurements are pivotal to models of star formation feedback & global galactic evolution.

2.5 Goal 4: Construct a Milky Way Template

[C II] 158 μm, the strongest Galactic cooling line, will be the premier diagnostic tool for studying external galaxies with far-infrared (FIR) observatories (SOFIA, Herschel) and in the submillimeter for galaxies with large redshifts (Atacama Large Millimeter Array). To interpret the measurement of extragalactic [C II] one must turn to the Milky Way for the spatial resolution needed to disentangle the various contributors to the total [C II] emission. At present, there is debate on the dominant origin of the [C II] emission in the Galaxy: diffuse H II regions, CNM clouds, or the surfaces of GMCs. STO-2 will solve this mystery. The [C II] and [N II] intensities depend on the strength of the UV heating and on the amount of gas in the appropriate ISM phase. The STO-2 mission covers a broad range of density and UV intensity, thus establishing the relationship between physical properties, [C II], [N II], CO, H I, FIR emission, and star formation. This study will provide the "Rosetta Stone" for translating the global properties of distant galaxies into reliable estimators of star formation rate and state of the ISM.

2.6 Possible Additional Balloon Missions

Balloon-borne missions have the great potential to be reflown to incorporate lessons from previous flights, install improved technology, and to explore additional scientific problems. The first flight STO-1 tested the technology and provided some initial [CII], [CI], and CO J=12-11 data. STO-2 is designed for the science described in previous sections and focuses on the Galactic disk between 3 kpc and 8.5 kpc. However, there are a number of extremely interesting scientific goals that could be met on subsequent balloon missions. These could either be a series of LDB flights like STO, or a possible ULDB mission, such as the Galactic/Extragalactic Ultra/Long Duration Balloon Spectroscopic Stratospheric Observatory (GUSSTO) mission in which many of this STO-2 team are involved. We briefly list here additional

scientific programs to give the flavor of this enormous potential.

Future balloon missions could map [C II] and [N II] in the very interesting center of the Galaxy. The compressed and turbulent interstellar medium of galactic nuclei provides a completely different environment for star formation than the relatively quiescent disk. The Galactic Center could be explored with sufficient spatial (∼3 pc) and spectral resolution to separate large clouds and trace material as it falls into and through the center region. This study could probe the origin of the mysteriously low [C II]/FIR flux ratio (Nakagawa et al., 1998), all of the center's massive cloud complexes, and the bar. High-velocity resolution observations will provide a new kinematic map of the gas, ultraviolet fields, and star formation in the nucleus.

The outer Galaxy and the nearby LMC galaxy provide a testing ground for understanding cloud formation and star formation in lower surface density and lower metallicity environments. Deep surveys of these regions with future missions could answer what determines the threshold in gas surface density which causes massive star formation to rapidly diminish.

One huge potential in future balloon missions will be to change wavelengths, and pursue other lines such as [O I] 63 μm. [O I] 63 μm increases in strength in dense gas and we envision deep surveys in regions selected by earlier missions such as STO-2. The [O I] maps will "light up" the regions of higher thermal pressures (or densities) and higher incident UV fields, like the surfaces of GMCs. Combined with the [C II] line, [O I] diagnoses key parameters of these star forming clouds.

GUSSTO, if approved, will provide some of this future science including: (i) the [OI] 63 μm line in addition to the [CII] and [NII] lines, (ii) using larger arrays to map a much more extended region of the Galaxy including the Galactic Center, and (iii) mapping the LMC galaxy. GUSSTO would launch ∼2017 so that STO-2 would provide a valuable scientific and technical precursor to GUSSTO. STO-2 would provide important data on source size and extent and the required sensitivities to detect [CII] and especially [NII] (which has had few prior detections). In addition, STO-2 would test new powerful local oscillators (LOs), a simpler, more rugged, and easier to align system for LO injection, and a new technique for beam splitting onto the multiple detectors, all of which are proposed for GUSSTO.

3 Science Requirements

The science goals outlined in Section 2 define a clear set of measurement requirements which the instrument and mission must be able to perform. Table 1 portrays this flow of requirements, setting the requirements for the instrument and mission implementations that are described in the sections to follow.

These requirements define the scope of the STO-2 Galactic Plane Survey, which will span a maximum of 35 square degrees at a modest sensitivity: 3σ detectability of 7×10^{-6} erg s^{-1} cm^{-2} sr^{-1} in [C II], adequate to detect the assembly of GMCs from diffuse CNM clouds with columns of a few times 10^{20} cm^{-2}. In [N II], sensitivity will be better than 2×10^{-6} erg s^{-1} cm^{-2} sr^{-1} with modest spectral and spatial smoothing, since diffuse HII regions will span many arcminutes on the sky even at a distance of 10 kpc. Such diffuse H II regions tend to dominate [N II] and [C II] emission from ionized gas (McKee & Williams, 1997) and are a substantial component of the ionized gas in the Galaxy. Previous surveys of [N II] and [C II] were limited to very small regions (KAO, ISO, Herschel) or had low angular resolution (COBE, BICE) (Bennett et al., 1994; Nakagawa et al., 1998). STO-2 will fully sample both species over large regions of sky to their diffraction limited resolution of $1'$.

Deeper coverage reaching truly diffuse cloud column densities corresponding to $A_V = 0.1$ mag and spanning the full emission scale height requires the STO-2 Deep Survey (DS). The Deep Survey is comprised of a series of 4-degree linear strips in Galactic latitude, spaced equally in Galactocentric radius, which include slices of the Molecular Ring, Scutum-Crux spiral arm, and inter-arm regions. These strips are chosen to match b strips made both by AST/RO (in [CI] and mid-J CO lines) and Mopra (in CO J=1-0). Deep surveys allow us to detect faint [CII] and [NII] from diffuse ionized clouds, probe the formation of small molecular clouds, and will determine the origin of most of the [CII] emission in the

Galaxy.

Table 1: ***Flow of Requirements, from Science goals to Instrument Implementation***		
Pertinent Science Goal(s)	**Measurement Requirement**	**Instrument requirement**
Life cycles (1), Formation of clouds (2)	Sufficient angular resolution to resolve ~3 pc clouds at the Molecular Ring (5 kpc)	1 arcminute resolution requires 0.8m aperture at 1-2 THz
Life Cycles (1), Formation of clouds (2), Galactic SFR (3), Milky Way template(4)	Sufficient spectral resolution to resolve spectral lines and measure cloud, shell and superbubble dynamics (km/s scale)	High resolution heterodyne spectroscopy with 1 km/s spectral channels
Life Cycles (1), Galactic SFR (3), Milky Way template (4)	Sufficient spectral bandwidth to encompass the Galactic rotation curve from l=305^o to 340^o	V_{LSR} = -140 to +20 km/s requires max 1 GHz bandwidth at [CII] frequency
Life Cycles (1), Galactic SFR (3), Milky Way template (4)	Sufficient mapping coverage to sample the inner Molecular Ring, interarm regions, and at least one major spiral arm	Mapping longitudes from l=305^o to 340^o and coverage of the molecular scale height (-0.5^o to 0.5^o) in latitude
Life cycles (1), Formation of clouds (2)	Sufficient sensitivity to sense CNM clouds aggregating into molecular clouds (limiting A_V = 0.4 mag)	3σ detectability of 1 K km/s = 7.1x10^{-6} erg/s/cm^2/sr in [CII]
Life cycles (1), Galactic SFR (3), Milky Way template (4)	Sufficient sensitivity to sense HII regions with emission measure of 50 cm^{-6} pc	3σ detectability of 0.3 K km/s = 1.0x10^{-6} erg/s/cm^2/sr in [NII] with spectral & spatial smoothing
Life Cycles (1), Formation of clouds (2), Galactic SFR (3)	Sufficient sensitivity and mapping coverage to cover the full [CII] and [NII] scale heights to A_V = 0.1 mag	Deep survey spanning -2^o to +2^o in latitude, with 3σ detectability of 0.3 K km/s = 2x10^{-6} erg/s/cm^2/sr in [CII]
Life Cycles (1), Formation of clouds (2), Galactic SFR (3), Milky Way template(4)	From prev. requirements, sufficient mapping speed to span 35 square degrees of mapping within one LDB flight from Antarctica	>1 sq.deg/day requires THz arrays of ~4 pixels per frequency band at current sensitivities (Trec=~1000K DSB)

4 Complementarity with Existing Data Sets and Other Missions

STO-2 will provide the community with a totally unique [C II] and [N II] survey, enabling quantitative extraction of many physical parameters of the interstellar medium in a 3D data cube. Its spatial resolution is comparable to Mopra surveys of CO emission in the southern hemisphere (see below) and also to the Southern Galactic Plane HI Survey (McClure-Griffiths, 2005), allowing placement of the [C II] 158 μm and [N II] 205 μm emission along the line of sight with respect to the CO and H I emission.

4.1 Relationship to Existing Data Sets

CO: The Mopra telescope in Australia has been upgraded for the STO project to make rapid CO surveys of the southern sky in all isotopologues of CO J=1-0. In 2011 we obtained maps in each isotopologue

from b = ±0.5° and l = 323° to 330°, at subarcminute spatial resolution and 0.1 km/s spectral resolution. We plan to map the region b = ±0.5° and l = 330° to 340° in 2012 with time recently awarded. A sample of our Mopra CO survey is shown in Figure 7. The CO J=1-0 surveys will complement the STO-2 survey by helping to identify molecular clouds whose surfaces STO-2 detects and whose ionized gas seen in [N II] and warm neutral gas seen in [C II] may be expanding into the ISM (Onishi et al., 2005). In addition, the STO team will obtain complementary CO J=4-3 and 7-6 maps at comparable resolution with NANTEN2 (see below, [C I] discussion).

H I: The STO-2 surveys enhance substantially the interpretation of existing H I surveys. The H I emission maps are sensitive only to column, whereas [C II] is sensitive to density times column. The [C II] therefore picks out the cloud regions with density > 30 cm^{-3}, whereas the H I is often dominated by the WNM emission (see Figure 5). In fact, H I clouds can appear in absorption, in emission or undetected against the confused background and foreground WNM. When H I and [C II] are both seen in emission, the ratio provides the gas density and pressure in the cloud. When extended and broad H I emission is seen without a [C II] counterpart, WNM or thermally unstable gas is identified.

[C I]: Moving from the CNM through the surfaces of molecular clouds to their cores, the predominant form of carbon transitions from C^+ to CO, with high abundances of C in the transition region. The STO team has access to guaranteed observing time at the NANTEN2 telescope in Chile to obtain complementary data for the regions covered by STO in the [CI] 370 μm and 609 μm lines with angular resolutions of 25 and 45 arcsec, respectively. In addition, a southern Galactic Plane survey of the 370 micron [CI] line (at 2' angular and 0.8 km/s spectral resolution) is currently being performed by the High Elevation Antarctic Terahertz (HEAT) telescope now in operation at 'Ridge A', the summit of the high Antarctic plateau (Kulesa et al. 2011). These data are in the public domain with no proprietary period. Maps from STO-2 coupled with CO and [C I] data, will follow carbon in all its forms in position, velocity, cooling rate, temperature and pressure as the interstellar gas evolves.

Infrared Continuum Surveys: MSX, Infrared Astronomical Satellite (IRAS), and Spitzer GLIMPSE and MIPSGAL Galactic plane surveys permit locating dark clouds, supershells, and star forming regions using the IR continuum.

4.2 Complementarity to Other Missions

STO-2 builds upon the heritage of three pioneering surveys which provided coarse pictures of [C II] and [N II] emission in the Galaxy. COBE (spatial resolution 7°, velocity resolution >1000 km/s), BICE (spatial resolution 15′, velocity resolution 175 km/s), and the Infrared Telescope in Space (IRTS, spatial resolution 10′, velocity resolution 750 km/s). *STO-2 has about the same sensitivity to surface brightness as these missions, but adds orders of magnitude in spatial and spectral resolution.* None of these missions had sufficient spectral or spatial resolution to locate clouds, or separate one cloud from another along a given line of sight, and thus could not draw specific conclusions about cloud properties or distributions, or even the origin of the [C II] or [N II] emission (Hollenbach & Tielens, 1999). Besides COBE, BICE and IRTS, other platforms include the former Kuiper Astronomical Observatory and Infrared Space Observatory, which did not survey the Galaxy in [C II] and [N II], but made pointed observations, albeit without sufficient spectral resolution to resolve the velocity structure of the lines. The Spitzer Space Telescope has no spectroscopic capability at these wavelengths.

The Herschel Space Observatory (HSO) is in its last year of operation and the observing program has been finalized. The high spectral resolution HIFI instrument on HSO has made a number of small maps of [CII] (and partly [NII]) emission from active star-forming cores and their adjacent cloud interfaces. The Herschel Galactic Observations of Terahertz C+ (GOT C+) project surveyed the Galactic disk in the [C II] line with HIFI's sub km/s resolution. GOT C+ measured 500 lines-of-sight (with a narrow 15 arcsec beam) separated typically by 0.5 to 1 degree. GOT C+ demonstrated the utility of velocity-resolved [C II] observations (together with complementary H I and CO surveys) to trace the different phases of the ISM. In particular, the GOT C+ survey found a significant number of dark gas components (Langer et al. 2010, Velusamy et al.

2010). STO-2 will map and measure the amount of this dark gas. Due to its coarse sampling, the GOT C+ survey lacks a picture of the surroundings of individual lines-of-sight, and STO-2 will provide the full picture of clouds forming and dissipating.

SOFIA with its present heterodyne instrument GREAT, and in particular with its future array heterodyne receiver upgrades, will be very efficient at mapping the detailed distribution and structure of ISM clouds at high spatial resolution and over small areas, but will not have sufficient observing time to conduct large scale mapping.

The STO-2 survey in the [C II] and [N II] lines will provide guidance to SOFIA follow-up studies of the small scale structure in confined areas of interest. STO-2 will be unique in providing maps of large areas at moderate spatial but full spectral resolution, thus obtaining an unbiased sample of ISM clouds and their motions across the Milky Way.

5 Science Implementation

STO-2 benefits tremendously from the experience gained on STO-1 and recent breakthroughs in THz LO technology by Co-I's at JPL. The STO-2 instrument package will be more sensitive, simple, and robust than on STO-1. The addition of a small, efficient, cryocooler will extend the mission's cryogenic lifetime to ~50 days. Except for the new LO's and cryocooler, all components are re-used from STO-1. The entire instrument package will pass through a stringent thermal-vac test before flight.

5.1 The 2012 STO-1 Campaign

Summary

STO was successfully launched on Jan. 15, 2012 (Figure 8). Science observations commenced within two hours of reaching float altitude (Figure 1b). They continued until an hour before mission termination on Jan. 29th. In its 14 day flight STO observed a number of star forming regions and made strip maps of the Galactic Plane in [CII], [CI], and CO J=12-11. During the mission the performance of all flight systems was fully characterized and adjustments made to the software as needed. After ~5 days a small vacuum leak developed in the flight cryostat that caused the cryogenic receivers to warm up prematurely. STO then entered its Warm Mission Phase, where it continued its observations of the Milky Way until termination.

Figure 8: STO being rolled-out for launch at Willy Field, Jan. 15, 2012.

Lessons Learned

STO-1 more than met its Minimum Mission Success criteria. In STO-2 we will achieve our Baseline Science Goals by benefiting from the following lessons–learned.

- **Carry back-ups of as many mission critical components as possible**. Within a few days of our first launch attempt the local oscillator (LO) for the [NII] receiver died, making it necessary to use a back-up unit. This unit did not produce enough output power to successfully pump the [NII] line, requiring us to observe the CO J=12-11 line instead. These were the only two LOs of this type available.
- **Thermal-vac test all flight systems for an extended period.** The STO dewar performed flawlessly until several days into the flight when what appears to have been a small vacuum leak occurred. This caused the cryogenic receivers to warm-up prematurely, ending [CII] and CO observations. We then

began the STO Warm Mission, observing with the ambient temperature [CI] receiver for the rest of the flight.

- **Design flight hardware to be as simple and modular as possible.** This is especially true for balloon payloads which are assembled and disassembled in the field. For STO-1 the complexity of instrument assembly was driven by the tight mechanical tolerances required of the THz optics. These tolerances also impacted instrument performance. Fortunately, for STO-2, new high-power LOs have been developed that greatly reduce these tolerances, making the assembly and performance optimization *much* easier.
- **Verify that target telemetry rates can be achieved regardless of gondola orientation.** During the STO flight it was only possible to achieve the desired high data rates if the gondola orientation was optimized for TDRSS.
- **System level testing cannot be overdone.** During flight a few software anomalies arose that were not detected during ground testing. Fortunately, we were able to correct for these. For STO-2 we have scheduled a longer I&T period to probe parameter space.

5.2 Instrument Summary

The observational goal of STO is to make high spectral (<1 km/s) and angular resolution (50") maps of the Galactic plane in [C II] (1.9 THz) and [N II] (1.46 THz). During the flight complementary maps in [CI] (492 GHz) will also be made. To achieve the angular resolution requirement STO utilizes a telescope with an 80cm aperture. To achieve the target spectral resolution and sensitivity, STO utilizes a leading-edge, THz heterodyne receiver system. The instrument portion of GUSSTO consists of (1) the telescope, (2) two- 4 pixel cryogenic receivers and one ambient temperature receiver (3) FFT spectrometers, (4) the instrument control electronics, and (5) the cryostat. The STO gondola is fully flight tested and contains (1) the solar arrays and power regulation system, (2) the attitude control system (ACS), (3) the gondola computer, (4) the solid-state memory for data storage, and (5) the transponder (provided by CSBF). Our observing strategy for the main survey is to make adjacent On-the-Fly (OTF) strip maps of the Galactic plane. An ambient load/cold-sky calibration (CAL) is used at the beginning and end of each strip map. During each strip map (lasting as long as ~20 minutes) the calibration load will be regularly observed. With this mode of operation, secondary chopping is not required.

5.2.1 System Description

A block diagram of the STO instrument is shown in Figure 9. The STO optical system consists of an f#20 Cassegrain telescope, Calibration (Cal) Box, Local Oscillator (LO) Box, and simple reimaging optics. The converging light from the telescope's secondary enters the Cal Box from above. Just inside the box is a flip mirror. When in the beam path the mirror redirects the light to a room temperature, Schottky receiver tuned to the 492 GHz [CI] line **(the same unit that was flown in STO-1)**. While on the ground this receiver is used to perform end-to-end testing of STO's electronics. It also provides ancillary science data while in flight. Once the on-board liquid helium supply is exhausted, the 492 GHz receiver continues to operate, allowing the possibility of a warm mission. While the pick-off mirror is in the beam path the mirror's back-side directs the light from a blackbody calibration load down into the cryostat. The calibration load can be heated or kept at ambient temperature. With the flip mirror out of the way, the telescope beam proceeds into the cryostat where it passes through a 10% reflective dielectric beam splitter used to inject the THz LO beams. **STO-2 utilizes recently developed LO's sources with ~10 times the power of those available at the time of the STO-1 flight. The ability to use a simple beamsplitter in STO-2 instead of the Fabry-Perot ring diplexer required by STO-1 dramatically reduces the complexity of the system, making assembly and optical alignment far simpler.** The new 1.9THz LO source was designed and built by our Co-I's at JPL specifically for STO. The beamsplitter and final multiplier stages are mounted to a plate maintained at 70K by a low-power cryocooler. **This cryocooler is also used to help cool the outer radiation shield of the cryostat, tripling the helium lifetime over what was achieved previously.** Once through the beamsplitter the combined sky and LO

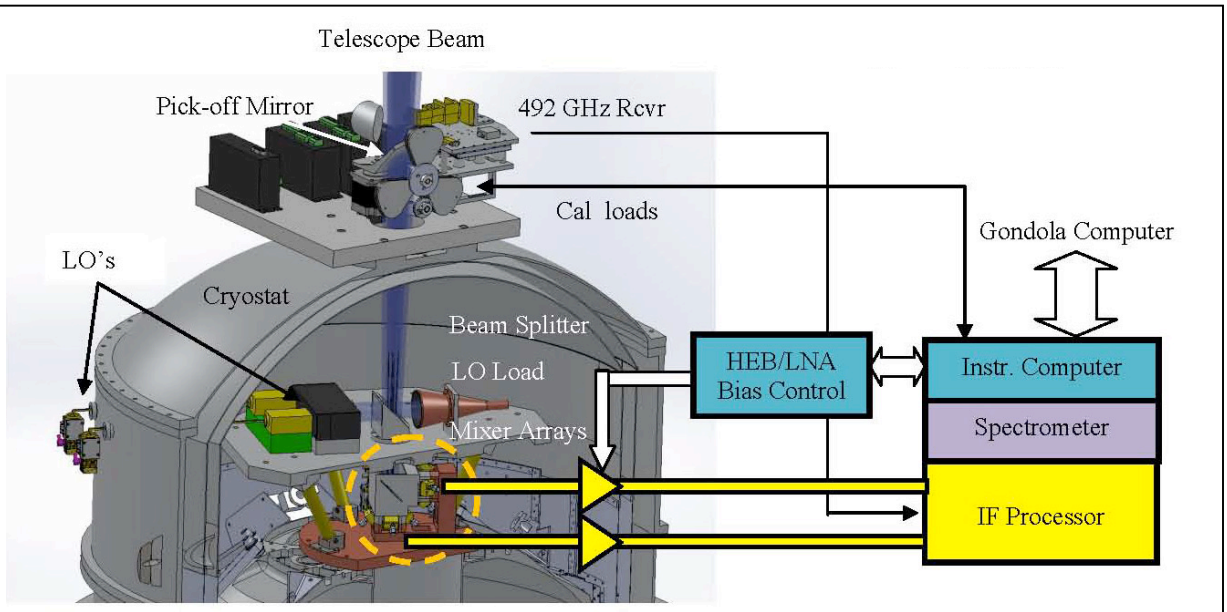

Figure 9: *STO-2 Instrument Block Diagram*

beams are split into horizontal and vertical components by a polarizing grid. One polarization reflects off the grid into reimaging optics that match the f#20 beams of the telescope to the beams needed to efficiently couple into the 1.45 THz mixer array. Similarly, the other polarization passes through the grid to reimaging optics that efficiently illuminate the orthogonally polarized 1.9 THz array. Each array has four Hot Electron Bolometer (HEB) mixers that are thermally strapped to the ~4K helium tank. These will be the same mixer arrays that flew in STO-1 and are the same type of mixers that are being flown in the high frequency band of the *Herschel* HIFI instrument.

The HEB mixers downconvert the high frequency sky signals to much lower, microwave frequencies. The mixers do this by multiplying the incident sky and LO beams together across a resistive nonlinearity in the HEB's micron-size superconducting bridge. The product of the multiplication contains sum and difference frequencies. Filtering permits only the difference or intermediate frequency (IF) signal to appear at the mixer output. From there coax conveys the downconverted sky signal to a series of low-noise cryogenic and room temperature microwave amplifiers. The amplifiers boost signal levels to where they can be digitized. The first stage IF low-noise amplifiers (LNAs) will utilize the same high-performance, low-power technology developed for STO-1. The IF signal will have a center frequency of 1.5 GHz and a 1 GHz bandwidth. At our highest observing frequency (1.9 THz, the [CII] line) a 1 GHz IF bandwidth will provide ~158 km/s of velocity coverage. Each GUSSTO pixel will have its own 1024 channel FFT spectrometer to produce a power spectrum of

Table 2: STO-2 Instrument Properties

Property	Description
Telescope	0.8m Cassegrain
Target Frequencies	[CI]: 1.9THz [[NII]: 1.46THz [CI]: 0.49THz
Angular Resolution	50 arc seconds @ [CII]
Receiver Type	2x2 HEB Mixer Arrays
System Noise Temp	~3000K (SSB)
Spectrometer	FFT
Spectrometer Bandwidths	1 GHz - Corresponds to 158 km/s for [CII]
Spectrometer Resolution	1 MHz – Corresponds to 0.3 km/s for [CII]
Cryogenic System	Hybrid He-4 Cryostat
Liquid Helium Hold-time	~50 days

the input signal. The power spectra from all 9 pixels are read by the instrument computer and passes on to the gondola via an ethernet link. Flight instrument electronics boxes house (1) the IF and spectrometer boards, (2) the LO-HEB/LNA bias board, (3) calibration flip mirror controller board, (4) instrument computer and (5) power conditioning-housekeeping boards. All these boards and subsystems successfully flew on STO-1.

5.2.2 Expected Sensitivity.

Recent lab measurements on waveguide and quasi-optical HEBs operating between 1 and 2 THz have yielded double side band (DSB) receiver noise temperatures of ~1000K. For our sensitivity calculations we have assumed an end-to-end receiver noise temperature of 1500K and single-sideband (SSB) system noise temperature, T_{sys} = 3000K. With the 13 second integration time per Nyquist-sampled resolution element characteristic of the unbiased, Galactic Plane survey (GPS) mode, we will be able to achieve rms noise levels of 0.33 K at a 1 km/s velocity resolution. The STO instrument properties are summarized in Table 2.

5.2.3 Component Selection

Technical Approach to Mixers and LNAs

STO-2 will utilize the same HEB mixers and low-noise amplifiers (LNAs) flown on STO-1. These mixers have been shown to have the sensitivity required for the STO-2 science investigations. The 2x2, 1.46 THz array was developed by JPL and the 2x2, 1.9 THz array by the University of Cologne. The LNAs were developed specifically for STO by Sander Weinreb at Caltech/JPL.

LO hardware 1.9 and 1.46 THz LO's

JPL has developed and delivered flight-qualified solid state local oscillator (LO) chains for HIFI that cover the 1400-1600 and 1600-1900 GHz bands. These LO chains consist of GaAs MMIC power amplifier modules and JPL designed and fabricated waveguide GaAs planar multiplier Schottky diode circuits. Since the development of HIFI, a number of improvements, in particular the capability of power combining in multiple chip multipliers has been demonstrated by JPL and will be used for STO-2.

A representative power curve for a 1.9 THz LO chains is shown in Figure 2. Both LO chains employ a x2x3x3 architecture. The first stage doubler in each chain utilizes a quad-chip configuration that allows it to handle input power levels in excess of 600 mW. The second stage is a dual-chip tripler. The final waveguide block contains a single tripler chip. A Potter horn will be used at the output. Even with a 10% beamsplitter being used for LO injection, each HEB pixel will receive ~1 microwatt of LO power, an ample amount for efficient mixing. **A lower power version of these LO chains was successfully flown on STO-1.**

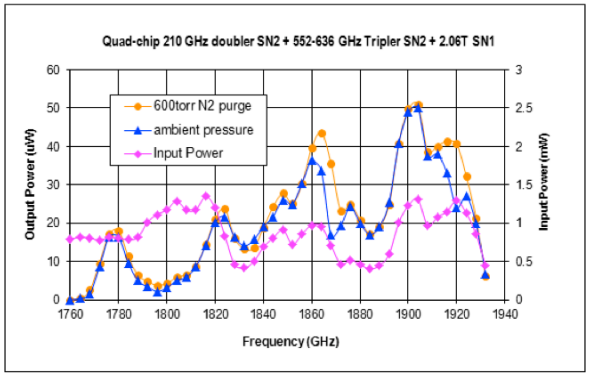

Figure 10: 1.9 THz LO Power curve.

The output beams from the two LO chains are orthogonally polarized. Each beam is transformed into four separate beams by a reflective phase grating and combined on a wire grid. These phase gratings and grids are the same types flown on STO-1. After the grid the LO and signal beams are combined on the beam splitter and travel down to the mixers.

Spectrometers

STO-2 will utilize the same spectrometer system successfully flown on STO-1. Developed originally for the PI's 64-beam 345~GHz heterodyne array (``SuperCam'') project by Omnisys, each spectrometer board has four 1 Gs, 8-bit digitizers and a Xilinx Virtex4 FPGA which together perform a real time FFT of the IF signal. The baseline spectrometer card has 2~GHz of total bandwidth and achieves excellent performance and stability. Four Omnisys boards are used in the flight system, providing 8 IF inputs with 1 GHz of bandwidth each. The demonstrated power dissipation of the complete 8 x 1 GHz spectrometer system is <100W. One additional spectrometer board will be mounted in the spectrometer pressure vessel for use with the Schottky receiver.

5.2.4 Cryostat

STO-2 will use the same high efficiency, 90 liter liquid helium cryostat from Ball Aerospace flown on STO-1, with the following enhancements:

1) A small, robust cryocooler will be added to extend the helium hold time to ~50 days.
2) A new vacuum collar and lid will be machined to simplify the integration of the instrument with the cryostat afforded by utilizing the new, high power LOs.

Figure 11 shows the STO cryostat mounted to its telescope. It has a 90 liter helium tank and an outer and inner vapor cooled radiation shield (OVCS and IVCS, respectively). Figure 1shows a cutaway view of the STO-2 cryostat. The STO mixer arrays and associated optics are mounted on the lower insert stage which is bolted to the top of the helium tank. The mixers dissipate approximately one milliwatt of heat and operate at $\leq$ 4.5 K. The IF output of each mixer is connected to an LNA via a short (~6 cm) length of stainless steel coax. The first stage of each LNAs dissipate ~2 mW. The LNAs and IVCS operate at 13 and 30 K, respectively, and are cooled primarily by the helium tank vent gas. Low-loss, AR-coated silicon and HDPE windows pass the desired signals from the telescope through the vacuum shell and vapor cooled shields. The ~100 GHz LO tones required to drive the frequency multipliers located on the 70K LO plate enter the cryostat through two waveguide vacuum windows in the side collar. Stainless steel waveguide and G-10 standoffs are used to thermally isolate the LO's from the 70K plate.

A cryocooler will be mounted on the side collar to provide additional cooling of the OVCS and LO plate. The cryocooler chosen is the Sunpower Cryotel CT, a low cost, commercial, linear Stirling cycle cooler. This cryocooler has 4.7 watts of capacity at 65 Kelvin, which is a margin of 50%. The cryostat model, shows that with a vacuum shell temperature of a 300 K and the lab verified STO-2 instrument heat loads, the helium hold time will be ~50 days.

On day 5 of the STO-1 flight a vacuum leak developed in the cryostat. The leak lead to the premature warm-up of the HEB mixers. Damage to the cryostat's shipping crate upon arrival at Willy Field suggests the leak could have been due to rough handling during transport to Antarctica. **Before the STO-2 hang test, the cryostat will undergo extensive thermal-vac testing.** After the hang test it will be packed in a padded, reinforced shipping container for the trip South.

Figure 11: STO Cryostat mounted to telescope (Payload #1, Willy Field, Dec. 2011)

5.3 Gondola & Telescope

5.3.1 STO Telescope

We will reuse the same telescope that was previously used for the first Antarctic flight of STO (Walker et al. 2010), shown in Figure 12, with only minor modifications. The primary mirror is an 80-cm diameter, f/1.5 hyperboloid made of honeycombed Ultra Low Expansion titanium silicate glass and weighing just 50 Kg. Its surface is polished to visible optical quality, therefore over-specified for imaging in the 100 to 200 μm range. Its support and spider arms are made of graphite-epoxy, which is light weight and has high thermal stability. For STO-2 the secondary mirror will be redesigned to provide a F/20 beam at the focal plane. We will also recoat the surface of the primary mirror.

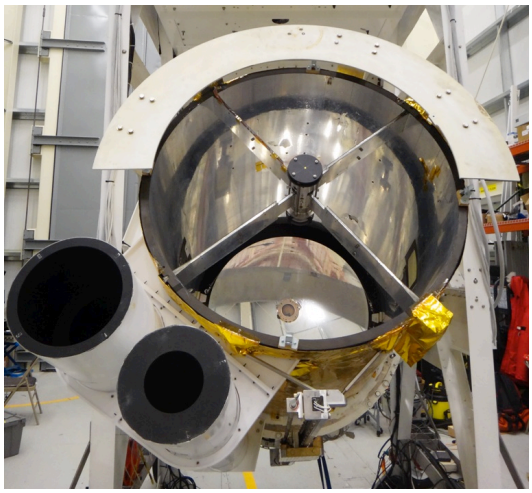

Figure 12: STO's 80-cm aperture telescope successfully flown in January 2012 from Antarctica. The two tubes on the lower left are the baffles of the two star cameras.

5.3.2 STO Gondola Structure

The STO gondola will be the same one previously used for STO-1. Figure 13 shows the STO gondola in full flight configuration. The gondola carries and protects the telescope and attached Dewar and detectors and houses the command and control systems for both STO and NASA-CSBF. Its basic dimensions (without solar arrays) are: 2 x 1.5 x 4.5 m (WxDxH). The frame is made of standard aluminum angles bolted together and painted with a white thermal coating. The structure is strong enough to support up to 2000 Kg even under the 10 g shock experienced at the end of the flight when the parachute inflates. The total mass of the STO payload, shown in Table 3, is well below the design structural limit. Additionally it is rigid enough to allow the required telescope pointing stability of < 15". The gondola can be separated into lighter components for easy post-flight retrieval in the field. NASA-CSBF balloon control electronics (the Support Instrument Package, SIP) is attached on the bottom of the gondola , inside a protective aluminum cage.

For STO-2 we will repair/replace the gondola structural components that were damaged during STO-1 Antarctic flight in January 2012. Subsequently we will perform thorough system & subsystems testing with a suspension system at APL's high-bay Balloon Payload Integration Facility, which is comparable to the balloon train.

Thermally all STO-1 subsystems behaved as predicted no major changes in the thermal design will be done for STO-2. We already have detailed thermal and structural analysis of the current gondola configuration. The models will be modified to take into account any small mechanical and electronics changes we plan for the STO-2 program.

Item	Weight lbs	Weight kg
Gondola frame & command & control	2100	953
Telescope:	490	222
Heterodyne spectrometer/He dewar:	360	163
CSBF equipment:	570	259
Total:	**3520**	**1597**

Table 3: STO-2 Weights

5.3.3 Command and Control System

Figure 14 gives an overview of STO-2 command and control system. It is virtually the same used for STO-1. We do not plan any modifications since it performed flawlessly during STO-1 flight. There are two main computers on-board: the Command and Control Computer (CCC) and the Actuators Control Computer (ACC). Both computers use a commercial ATX motherboard with a Pentium-based CPU, solid state hard drives, and Linux as the operating system. They are housed in two vessels that maintain 1 atm pressure throughout the flight, allowing the use of off-the-shelf commercial grade electronic

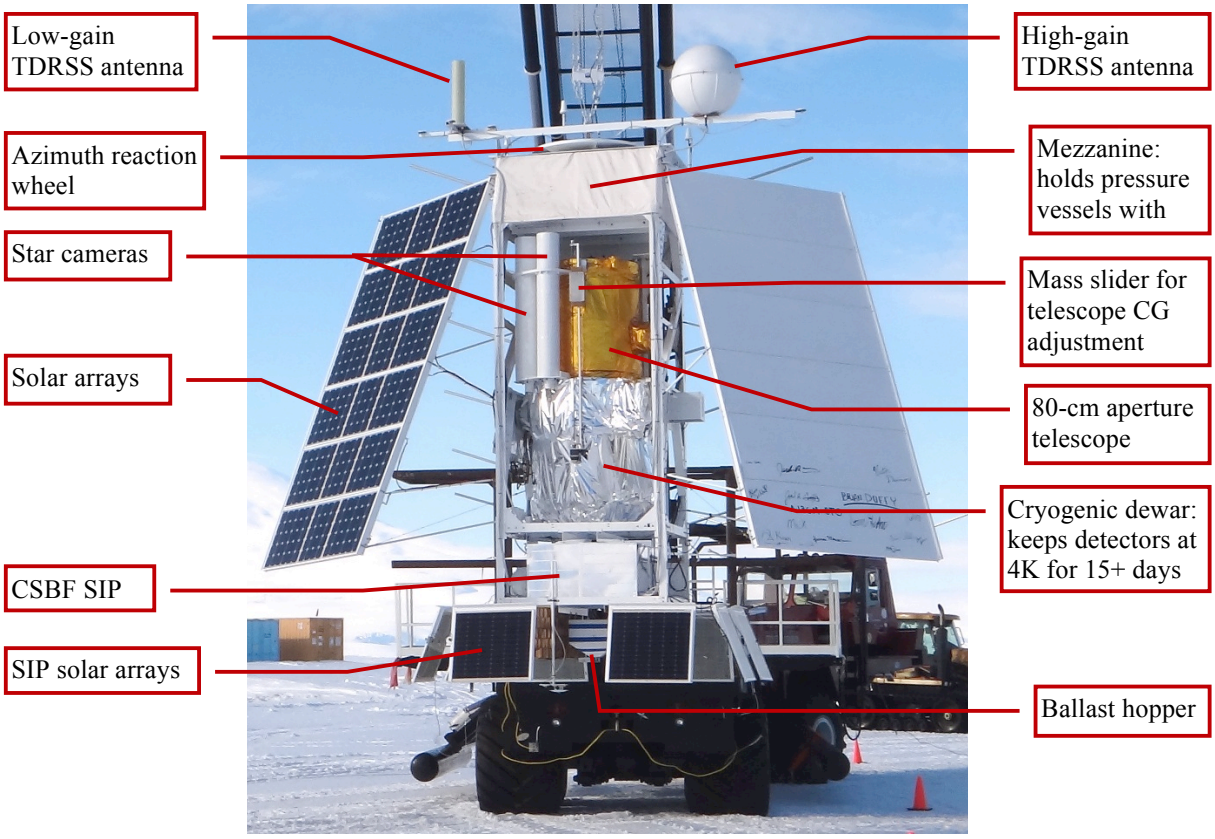

Figure 13: The STO-1 gondola ready for its first scientific flight from Antarctica in January 2012.

components. The CCC is responsible to schedule all the operations performed by the gondola and handles the communications between the gondola subsystems and the ground. It also communicates to the science computer via an Ethernet socket. It can operate fully autonomously or execute commands received from the ground. The ACC acts as interface between the CCC computer and all the other gondola subsystems. It gathers all the housekeeping data (temperatures, pressures, voltages …) and sends them to the CCC for delivery to the ground. The ACC also handles the attitude control system described further below.

5.3.4 Telecommunications

The telecommunications system for STO-2 will be exactly the same succesfully used for STO-1. We will rely entirely on the NASA-CSBF provided Support Instrument Package (SIP) for the remote link between the gondola and the ground. The SIP has three available channels to/from the ground. For the first ~24 hours the gondola will be in Line-of-Sight (LOS) to the launch station in Antarctica and will use a UHF radio link at a data rate of 1 Mb/s. During LOS operations ample amounts of housekeeping data will be available for analysis of both science and gondola performance. After loss of the LOS radio link, communications will be maintained via a 92-Kb/s TDRSS

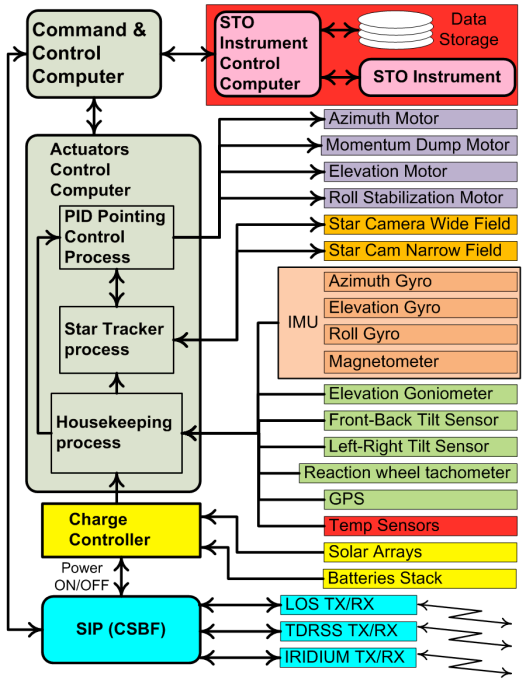

Figure 14: Gondola subsystems block diagram.

satellite relay and a lower rate IRIDIUM relay (one 255 bytes packet every 15 minutes). A 6-Kb/s TDRSS link is also available and is used as backup. TDRSS and IRIDIUM signals will be received at CSBF's Operations Control Center (OCC) in Palestine (TX) and sent to a local STO ground support computer that will redistribute the data packets to other STO ground stations at APL, the University of Arizona and to the team in Antarctica. All the STO ground stations will be able to display and store the same telemetry information received at the OCC, and commands can be sent to the gondola computers from any station. About 90% of the science data acquired during the flight will be downlinked using the TDRSS link and will be sufficient to meet the scientific goals in the case of loss of the payload. The ground support computers will use the same software package GSEOS, by GSE Software, Inc., that was previously used for STO-1.

5.3.5 Pointing System

Also the pointing system will be virtually the same used for STO-1 with the addition of a roll compensation system (described below). The science pointing requirements are: pointing range of 360° and 0 to 57° in elevation less a half cone of 20° in the direction of the Sun; stability < 15"; knowledge < 15"; source acquisition accuracy < 20". During the STO-1 Antarctic flight we have demonstrated that the current design exceeds those requirements.

To aim the telescope at the desired target in the sky we use an elevation/azimuth mount. The telescope is attached to the gondola on its elevation axis and a torque motor attached to it rotates the telescope in elevation by pushing against the gondola frame. It is also equipped with a goniometer that measures the angle with respect to the gondola with a resolution of ~ 10 arc minutes. To point in azimuth the entire gondola rotates on the vertical axis via Momentum Transfer Unit (MTU) which is same as the one flown in STO-1. It uses the same type of torque motor as the elevation to act against a large moment of inertia reaction wheel (RW) to provide steering torque to the gondola. The balloon suspension point is connected through a thrust bearing allowing the gondola to rotate independently about the balloon cable. The RW is slowed by applying a constant braking torque against the balloon cable which is a torsionally stiff ladder. The braking is achieved by constantly closing the connection of a short-circuit load to a separate torque motor, acting as a generator, connected between the balloon suspension and the RW. The braking regulates the maximum speed of the RW. With STO this technique of constantly transferring momentum to the balloon suspension yielded excellent torque control and prevented the RW to spin too

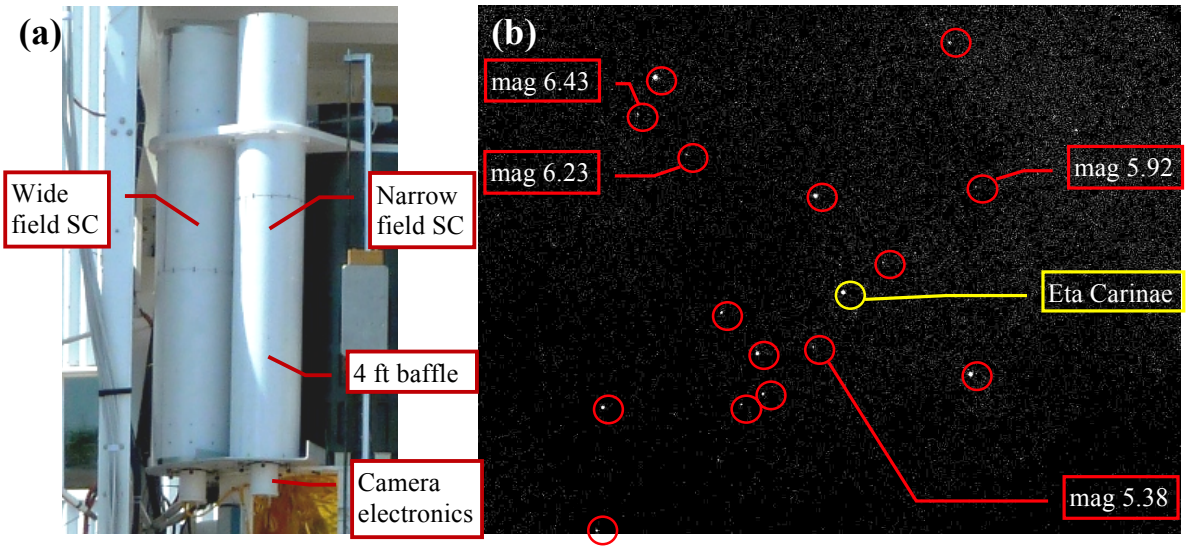

Figure 15: (a) STO-1 Star cameras are the same used for STO-2. (b) Eta Carinae star field imaged by STO's wide field star tracker during STO-1 Antarctic flight at 120kft altitude (jpeg compressed). Red circles indicate stars identified by the star recognition algorithm. Position knowledge: 1 arcsec

fast.

During STO-1 flight we detected a side-to-side pendulation (roll) of the gondola with fast frequency of about 0.5 Hz and amplitude between 30 and 150 arc seconds. This roll translates in an azimuth pointing error of the telescope in the sky given by the formula: *Roll_amplitude * sin(Telescope_elevation)*, which becomes significant for high telescope elevations. In STO-1 the only way to compensate for the roll induced error was to fast dither the gondola in azimuth. However, due to the large gondola inertia and the high roll frequency, it was extremely hard to completely eliminate this pointing error source. For STO-2 we will implement an active roll stabilization system that will remove the fast components of the gondola roll. The system is basically a side-mounted MTU without the momentum dump mechanism: a motor connected to the back of the gondola frame that torques on a vertically mounted wheel. The hardware and servo control system is basically the same as the one for the MTU. Analytical and small scale model simulations of the gondola fast roll oscillation show that the planned active roll compensation system will be very effective in removing the fast frequency roll oscillations.

The fine gondola attitude is determined by an Inertial Measuring Unit (IMU) and two APL built star trackers. The IMU maintain measurement of the telescope azimuth and elevation position at sub-arcsecond precision at a rate of 200Hz. It is composed of three high-precision, low-drift fiber optic gyroscopes, the Optolink SRS-2000. These gyroscopes have a bias drift of less than 3 arcmin/hr over a wide temperature range and less than 18 arcsecs/hr at a fixed temperature. The gyroscopes angle random walk is less than 1.08 arcsec/√hr. They are mounted on 3 orthogonal faces of a precision machined cube which is attached to the telescope metering structure. Initialization of azimuth and elevation for the IMU is done on the ground before launch. From the STO-1 flight experience, when the gondola reaches float altitude, the initial error in estimating telescope orientation will be < 30 arc minutes.

For precision attitude knowledge to < 5 arcseconds STO-2 flies the same two star cameras developed and built by APL for the STO1 program, and successfully used on STO-1 Antarctic flight (see Figure 15). They are also attached to the telescope metering structure. They are commercial Stardot Netcam SC-5 with APL modified hardware to allow them to operate at float altitude environment. One star camera is configured with a 50mm focal length f/2.4 lens and red filter. It has a ~7° FOV and is capable of detecting magnitude 6.5 (and dimmer for red stars) stars at altitude during daylight conditions. The

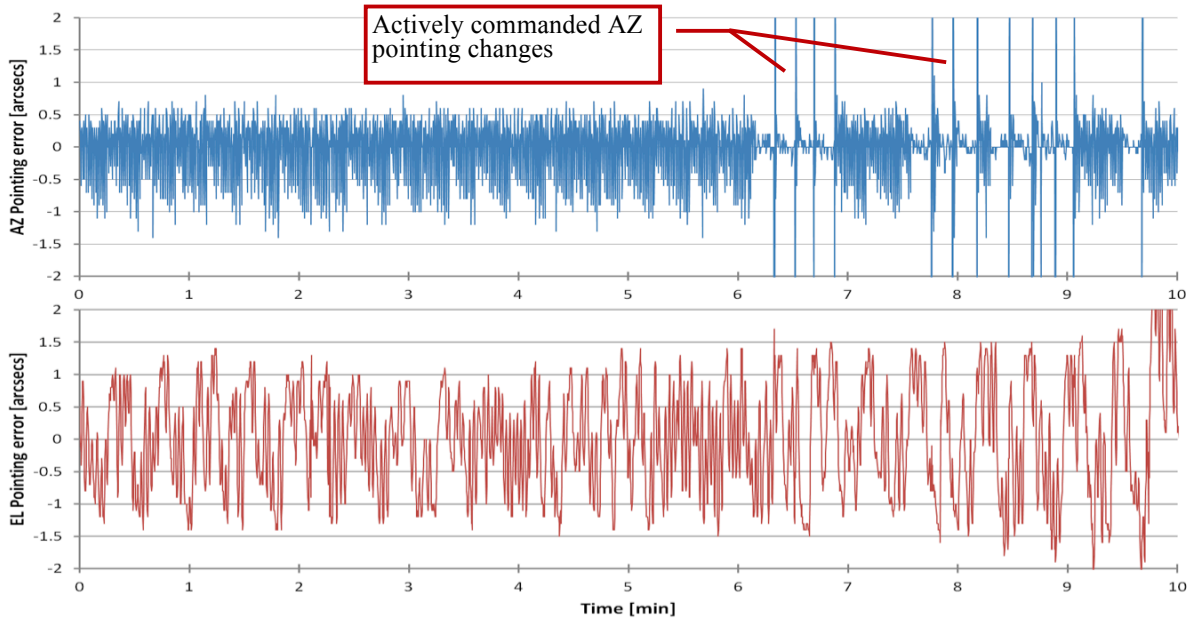

Figure 16: Example of typical Azimuth and Elevation pointing errors achieved during STO-1 Antarctic flight.

camera's FPGA is loaded with an APL custom configuration that performs image flat fielding. The camera's processor computes spot centroids and provides a timestamp for each captured image. The results are sent via Ethernet to the pointing control process on the ACC computer that performs star identification and calculates the boresight aim direction. During STO-1 flight the star camera position knowledge accuracy was better than 2 arc seconds (see Figure 16).

STO's second star camera is identical to the first except that the lens is a 500mm mirror lens. It has a ~0.5° FOV and is capable of imaging bright stars (< magnitude 2), and planets during daylight from the ground. It is used for testing and calibration of the pointing control system from the ground in daylight conditions like in Antarctica where the Sun is up 24/7. In-flight it will be used as a guide telescope to lock onto the target star and for establishing absolute error limits on the wide-field star camera pointing solution. Lastly, it can also be used to provide absolute position references in the event that there is a problem with the wide-field star camera provided that rough pointing is known.

The digital pointing control system will be the same successfully used for STO-1. It uses a Proportional-Integral-Derivative (PID) controller to determine motor drive current entirely from position error sensors. Each pointing mode has four control coefficients per axis that can be adjusted in flight for optimum performance. The pointing performance achieved during STO-1 flight (see Figure 16) demonstrates that the combination of gyroscopes, star trackers and PID controller delivers a pointing knowledge of about 2 arc-seconds and a pointing stability of < 2 arc-seconds in both elevation and azimuth, fully meeting the requirements for STO-2.

5.3.6 Power System

The STO-2 power system will be the same used for STO-1 with no modifications planned since it performed flawlessly during the Antarctic flight. It consists of the solar arrays, the charge controller, and the battery stack. The solar arrays are composed of 480 cells model A300 from SunPower Corp. The maximum power delivered by the arrays is about 1100 W, while the estimated total STO power requirement will be only about 450 W. This gives a margin of 650 W. We estimate that during landing and recovery of STO-1 we lost about 50% of the arrays. For STO-2 we plan to replace only the damaged arrays. The new arrays are assembled by SunCat Solar of Arizona who also built the ones for STO-1. The charge controller distributes the load across the panels, ensures that the system's battery stacks are maintained at near full charge, sunlight permitting, and provides on/off power switching capability from ground commands. It will be the same used for STO-1 and will require no modifications.

The battery stack is composed of 2 sealed lead-acid ODISSEY PC1700 rechargeable batteries connected in series. The stack has a capacity of 65 amp-hours with a nominal bus voltage of 24 V. During the STO-1 flight the battery charge level never dipped below 60%.

5.4 Data Analysis and Archiving

STO-2 data analysis will make use of the data reduction techniques developed for STO-1. Both missions benefit from the many man-years of effort put into reducing Herschel/HIFI HEB receiver data. Indeed, several of our team members (including Chris Martin, Jorge Pineda, and team members from U. Cologne) are experts in this area and are now applying their skills to the STO-1 data set. Once the raw data has been accurately tagged and a baseline removed, a wide range of standard data reduction packages and techniques can be employed. We plan to adopt an OTF data reduction scheme similar to that developed at FCRAO, whereby coadded and regridded data is written as FITS & CLASS files, and headers for each scan are written into a MySQL relational database. This approach facilitates efficient logging and retrieval of the data. The most demanding storage requirement for a 35 sq. degree spectral map is 10 GB. In flight this data volume can be readily handled by embedded computers with nonvolatile FLASH memory. The spatially & spectrally regridded final data product encompasses <500 MB. While the entire science team will be involved in analysis and interpretation of STO-2 data in Spring 2015, near-immediate access of these data products to the greater scientific community will be provided through a web browser interface that interfaces with MySQL and the FITS data cubes. There will be two data

product releases in the proposal performance period: (1) a preliminary, first light, release after the Antarctic mission in March 2015, and (3) a final release of all data in December 2015. The final release will be fully calibrated and include all science products. All science tools, packaged reduction software, data products and catalog products will be made available from the STO survey web page.

6 Management

The STO-2 project brings together an experienced team of researchers from 8 institutions; the University of Arizona, Johns Hopkins Applied Physics Laboratories, SETI Institute, Jet Propulsion Laboratory, Caltech, Smithsonian Astrophysical Observatory, Univ. of Maryland, Oberlin College, and the University of Cologne. These organizations and individuals have successfully collaborated on STO-1 as well as a wide variety of other projects and look forward to making STO-2 and the science it will produce a reality.

6.1 Project Management & Organization

The organizational structure of STO-2, shown in Figure 21, closely follows that of STO-1. It is designed to provide effective control of the project while allowing delegation of authority to be made at the proper level within the team. Dr. Walker (PI) is responsible for all aspects of the success and scientific integrity of STO-2. He will be assisted at the University of Arizona by Dr. Craig Kulesa, who will serve as Deputy PI and Brian Duffy, Project Manager (PM). The STO science team will be led by Dr. David Hollenbach (SETI Institute) who will be STO Project Scientist (PS). The Instrument Team will be led by the PI (Walker). Dr. Bernasconi (APL Institutional PI) will oversee the STO gondola efforts at APL. Dr. Jonathan Kawamura will oversee the FPU integration and test at JPL. The FPU will re-use flight tested 1.46 THz mixers from JPL and 1.9 THz mixers from the University of Cologne. Prof. Juergen Stutzki and Dr. Patrick Puetz will oversee STO-2 science and instrumentation efforts, respectively, at the University of Cologne. As with STO-1, the team will make extensive use of electronic communication and management tools including e-mail, secure websites, on-line meetings and video communications to expedite accurate information dissemination. All pertinent management and control information will be posted on a secure STO website maintained by the UofA and available to all participants. These tools will be used in daily interactions as well as in weekly team telecons and monthly status briefings to ensure that major issues are visible to and addressed by all affected team members. In addition, face-to-face team meetings will be conducted when appropriate, often in conjunction with program milestones.

6.2 Master Schedule

The master schedule shown in Figure 17 identifies the project's major milestones and development activities. **We are fortunate in that all flight critical systems were recovered from STO-1 in excellent condition**. Indeed, a careful inspection of flight hardware in the hangar after recovery revealed no significant damage, only a few gondola structural members and cabling cut during recovery operations need be replaced. The flight cryostat, optics, and critical electronic systems (including the spectrometer and telescope control computer) were flown back by commercial air and have undergone evaluation in the lab. The cryostat, except for the vacuum leak that occurred in flight, appears to be in excellent shape and the electronics ran when powered-up. This successful recovery allows STO-2 to get off to a running start

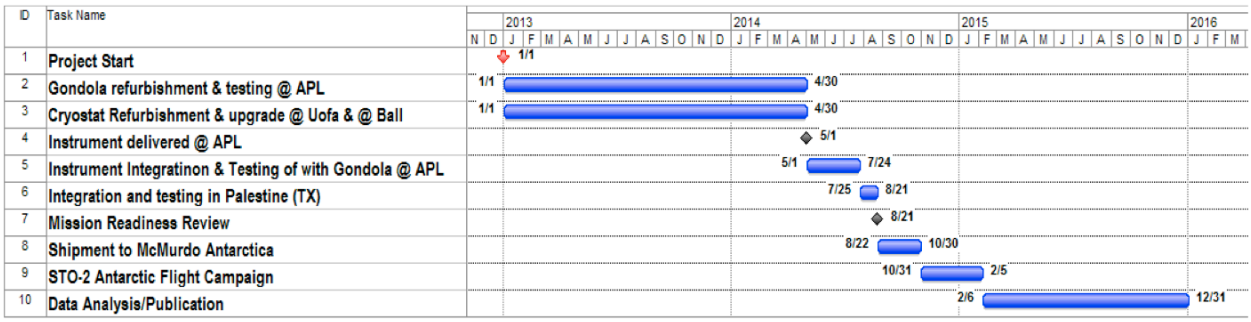

Figure 17: STO-2 Master Schedule

on January 1, 2014. The first year's efforts at APL will focus on the full reassembly and testing of the gondola/telescope. The Uof A will work with Ball Aerospace to refurbish and upgrade the flight cryostat. JPL and ASU will integrate new, high-power THz LO's into the instrument. These LO's will greatly simplify the optical system, making the instrument more sensitive, robust, and easy to work on in the field. In early 2014 on-the-sky tests of the gondola/telescope will be performed at APL using a CO J=1-0 receiver previously used for similar tests on STO-1. During this same period the fully tested FPU will be brought to the UofA for I&T with the upgraded flight cryostat. The I&T will include an extensive thermal-vac test using facilities at the UofA (or Raytheon Inc.). In May 2014 the fully characterized flight instrument/cryostat will be shipped to APL for I&T with the gondola/telescope. Full system tests will be carried out at APL through July 2014, ending with a Payload Readiness Review (PRR). Following the successful PRR, STO-2 will be shipped to Palestine in July-August 2014 for a hang-test/compatibility check with CSBF's balloon control and communication equipment. Following the hang-test we will have a Mission Readiness Review that will clear STO-2 for an Antarctic flight. After the successful MRR, STO-2 will be shipped to McMurdo in September 2014. The flight support team members will deploy to McMurdo in late Oct. 2014 to prepare STO-2 for the Antarctic flight. The window for flight operations is December 2014 through January 2015. Science data reduction and analysis will start immediately after conclusion of flight operations.

References

Bania, T. M., Lockman, F. J. 1984, "A survey of the latitude structure of galactic H I on small angular scales", ApJS, 54, 513

Bennett, C. L., et al. 1994, "Morphology of the interstellar cooling lines detected by COBE", ApJ, 434, 587

Bernasconi, P. N., Rust, D. M., Eaton, H. A. C., Murphy, G. A. A., 2000, "A Balloon-Borne Telescope for high resolution solar imaging and polarimetry", in "Airborne Telescope Systems", Ed. by R. K. Melugin, and H. P. R¨oser, SPIE proceedings, 4014, 214

Bernasconi, P. N., Eaton, E. A. C., Foukal, P., Rust, D. M., 2004, "The Solar Bolometric Imager", Adv. Space. Res., 33, 1746

Boreiko, R.T. & Betz, A.L. "The 12C/13C Isotopic Ratio in Photodissociated Gas in M42", ApJL, 467, L113

Dame, T. M., Hartmann, D., Thaddeus, P., 2001, "The Milky Way in Molecular Clouds: A New Complete CO Survey", ApJ, 547, 792

de Avillez, M. A., & Breitschwerdt, D. 2005, "Testing Global ISM Models: A Detailed Comparison of O VI Column Densities with FUSE and Copernicus Data", ApJL, 634, L65

Elmegreen, B. G. 1996, "What Do We Really know About Cloud Formation" in Unsolved Problems of the Milky Way, 169, 551

Engargiola, G., Plambeck, R. L., Rosolowsky, E., & Blitz, L. 2003, "Giant Molecular Clouds in M33. I. BIMA All-Disk Survey", ApJS, 149, 343

Gao, J. R., Hajenius, M., Baselmans, J., Klawijk, P., de Korte, Voronov, B., and Gol'tsman, G., 2004, "NbN Hot Electron Bolometer Mixers with Superior Performance for Space Applications", International Workshop on Low Temperature Electronics, 23-24 June 2004, (invited paper).

Gazol, A., V´azquez-Semadeni, E., & Kim, J. 2005, "The Pressure Distribution in Thermally Bistable Tur-bulent Flows", ApJ, 630, 911

Grenier, I. A., Casandjian, J.-M., & Terrier, R. 2005, "Unveiling Extensive Clouds of Dark Gas in the Solar Neighborhood", Science, 307, 1292

Heiles, C., & Troland, T. H. 2003, "The Millennium Arecibo 21 Centimeter Absorption-Line Survey. II. Properties of the Warm and Cold Neutral Media", ApJ, 586, 1067

Hennebelle, P., & P´erault, M. 2000, "Dynamical condensation in a magnetized and thermally bistable flow. Application to interstellar cirrus", A&A, 359, 1124

Heyer, M. H., Brunt, C., Snell, R. L., Howe, J. E., Schloerb, F. P., Carpenter, J. M., 1998, "The Five College Radio Astronomy Observatory CO Survey of the Outer Galaxy", ApJS, 115, 241

Heitsch, F., Slyz, A. D., Devriendt, J. E. G., Hartmann, L. W., & Burkert, A., 2006, "The Birth of Molecular Clouds: Formation of Atomic Precursors in Colliding Flows", ApJ, 648, 1052

Hollenbach, D. J., Tielens, A. G. G. M. 1999, "Photodissociation regions in the interstellar medium of

galaxies", RvMP, 71, 173

Hu, Q., Williams, B. S., Kumar, S., Callebaut, H., Kohen, S., & Reno, J. L. 2005, Semiconductor Science Technology, 20, 228

Hunter, D. A., Elmegreen, B. G., van Woerden, H. 2001, "Neutral Hydrogen and Star Formation in the Irregular Galaxy NGC 2366", ApJ, 556, 773

Jenkins, E. B., & Tripp, T. M. 2011, ApJ, 734, 65

Juvela, M., Padoan, P., & Jimenez, R. 2003, "Photoelectric Heating and [C II] Cooling in Translucent Clouds: Results for Cloud Models Based on Simulations of Compressible Magnetohydrodynamic Turbu-lence" ApJ, 591, 258

Kennicutt, R. C. Jr. 1989, "The star formation law in galactic disks", ApJ, 344, 685

Kim, W.-T. & Ostriker, E.C. 2002, "Formation and Fragmentation of Gaseous Spurs in Spiral Galaxies". ApJ, 570, 132

Kim, W.-T. & Ostriker, E.C. 2007, "Gravitational Runaway and Turbulence Driving in Star-Gas Galactic Disks". ApJ, 646, 213

Kritsuk, A. G., & Norman, M. L. 2002, "Thermal Instability-induced Interstellar Turbulence", ApJL, 569, L127

Kulesa, C.A., Walker, C.K., Young, A.G., Ashley, M.C.B., & Storey, J.V.W. 2011, "HEAT: The High Elevation Antarctic Terahertz telescope". Proceedings of the 22nd International Symposium on Space Terahertz Technology, paper 9-3.

Kulkarni,S. R., & Heiles, C. 1987, "The atomic component", ASSL Vol. 134: Interstellar Processes, 87

Kwan, J., Valdes, F. 1987, "The spatial and mass distributions of molecular clouds and spiral structure",ApJ,315, 92

Langer, W. D., Velusamy, T., Pineda, J. L., et al. 2010, "C^+ detection of warm dark gas in diffuse clouds" ,A&A, 521, L17

Linsky, J. L., and 16 colleagues 2006. What Is the Total Deuterium Abundance in the Local Galactic Disk?. Astrophysical Journal 647, 1106-1124.

Mac Low, M.-M., Balsara, D. S., Kim, J., & de Avillez, M. A. 2005, "The Distribution of Pressures in a Supernova-driven Interstellar Medium. I. Magnetized Medium", ApJ, 626, 864

Martin, C. L., Kennicutt, R. C. Jr 2001, "Star Formation Thresholds in Galactic Disks", ApJ, 555, 301

Martin, C. L., Walsh, W. M., Xiao, K., Lane, A. P., Walker, C. K., and Stark, A. A. 2004, "The AST/RO Survey of the Galactic Center Region. I. The Inner 3 Degrees", ApJS, 150, 239.

McClure-Griffiths, N. M. etal 2005, "The Southern Galactic Plane Survey: H I Observations and Analysis", ApJS, 158, 178

McKee, C. F. 1989, "Photoionization-regulated star formation and the structure of molecular clouds", ApJ, 345, 782

McKee, C. F., Ostriker, J. P. 1977, “A theory of the interstellar medium - Three components regulated by supernova explosions in an inhomogeneous substrate”, ApJ, 218, 148

McKee, C. F. Williams, J. P. 1997, “The Luminosity Function of OB Associations in the Galaxy”, ApJ, 476, 144

Mueller, E. and Waldman, J., 1994, “Power and Spatial Mode Measurements of Sideband Generated Spatially Filtered, Submillimeter Radiation”, MTT, 42, No. 10, 1891.

Mueller, E., Coherent Inc., Private Communication.

Nakagawa, T., Yui, Y. Y., Doi, Y., Oku da, H., Shibai, H., Mochizuki, K., Nishimura, T., & Low, F. J. 1998, “Far-Infrared [C II] Line Survey Observations of the Galactic Plane”, ApJS, 115, 259

Neufeld, D. A., Green, J. D., Hollenbach, D. J., Sonnentrucker, P., Melnick, G. J., Bergin, E. A., Snell, R. L., Forrest, W. J., Watson, D. M., Kaufman, M. J. 2006. Spitzer Observations of Hydrogen Deuteride. Astrophysical Journal 647, L33-L36.

Onishi, T. et al., 2005, “New View of Molecular Gas Distribution of the Southern Sky: CO Surveys with NANTEN”, in Protostars and Planets V, LPI Contribution No. 1286., p.8301

Ostriker, E. C., & Kim, W.-T. 2004, ASP Conf. Ser. 317: “Milky Way Surveys: The Structure and Evolution of our Galaxy”, 317, 248

Ostriker, E. C., McKee, C. F., & Leroy, A. K. 2010, ApJ, 721, 975

Parravano, A., Hollenbach, D. J., McKee, C. F. 2003, “Time Dependence of the Ultraviolet Radiation Field in the Local Interstellar Medium” ApJ, 584, 797

Piontek, R. A., & Ostriker, E. C. 2005, “Saturated-State Turbulence and Structure from Thermal and Mag-netorotational Instability in the ISM: Three-dimensional Numerical Simulations” ApJ, 629, 849

Planck Collaboration, Ade, P. A. R., Aghanim, N., et al. 2011, A&A, 536, A19

Schmidt, M. 1959, “The Rate of Star Formation”,. ApJ, 129, 243

Steiman-Cameron, T. Y., Wolfire, M., & Hollenbach, D. 2010, ApJ, 722, 1460

Taylor, A. R. et al 2002 in “Seeing Through the Dust: The Detection of HI and the Exploration of the ISM in Galaxies”, Ed. by A. R. Taylor, T. L. Landecker, and A. G. Willis, (ASP:San Francisco), 68

Taylor, A. R. et al 2003, “The Canadian Galactic Plane Survey”, AJ, 125, 3145

Tilanus, R. P. J., Allen, R. J., 1991, “Spiral structure of M51 - Distribution and kinematics of the atomic and ionized hydrogen” A&A, 244, 8

Ulich, B.L., & Haas, R. W., 1976, “Absolute calibration of millimeter-wavelength spectral lines”, ApJs 30, 247

Vastel, C., Polehampton, E. T., Baluteau, J.-P., Swinyard, B. M., Caux, E., Cox, P. 2002. Infrared Space Observatory Long Wavelength Spectrometer Observations of C^+ and O^0 Lines in Absorption toward Sagittarius B2. Astrophysical Journal 581, 315-324.

Velusamy, T., Langer, W. D., Pineda, J. L., et al. 2010,”[C II] observations of H_2 molecular layers in

transi-tion clouds", A&A, 521, L18

Wiklind, T., Rydbeck, G., Hjalmarson, A., Bergman, P., 1990, "Arm and interarm molecular clouds in M 83", A&A, 232, 11

Williams, J. P., McKee, C. F. 1997, "The Galactic Distribution of OB Associations in Molecular Clouds", ApJ, 476, 166

Wolfire, M. G., McKee., C. F., Hollenbach, D., Tielens, A. G. G. M. 2003, "Neutral Atomic Phases of the Interstellar Medium in the Galaxy", ApJ, 587, 278

Wright, E. L. et al 1991, "Preliminary spectral observations of the Galaxy with a 7 deg beam by the Cosmic Background Explorer (COBE)", ApJ, 381, 200

Zhang, X., Lee, Y., Bolatto, A. D., and Stark, A. A. 2001, "CO (J=4-3) and [C I] Observations of the Carina Molecular Cloud Complex", ApJ, 553, 274.